NASA TECHNICAL MEMORANDUM

NASA TM X-1372

NASA TM X-1372

DESIGN AND FABRICATION OF NONCONDENSING RADIATOR FOR ENVIRONMENTAL EVALUATION OF SPACE POWER MERCURY RANKINE SYSTEM

by

William T. Wintucky and Lawrence A. Mueller

Lewis Research Center

and

John W. Cox and Harold H. Greenfield

Lockheed Missiles and Space Company

NATIONAL AERONAUTICS AND SPACE ADMINISTRATION • WASHINGTON, D. C. • MAY 1967

NASA TM X-1372

DESIGN AND FABRICATION OF NONCONDENSING RADIATOR FOR ENVIRONMENTAL EVALUATION OF SPACE POWER MERCURY RANKINE SYSTEM

By William T. Wintucky and Lawrence A. Mueller

Lewis Research Center
Cleveland, Ohio

and

John W. Cox and Harold H. Greenfield

Lockheed Missiles and Space Company
Sunnyvale, Calif.

NATIONAL AERONAUTICS AND SPACE ADMINISTRATION

For sale by the Clearinghouse for Federal Scientific and Technical Information
Springfield, Virginia 22151 – CFSTI price $3.00

DESIGN AND FABRICATION OF NONCONDENSING RADIATOR FOR ENVIRONMENTAL EVALUATION OF SPACE POWER MERCURY RANKINE SYSTEM

by William T. Wintucky, Lawrence A. Mueller, John W. Cox* and Harold H. Greenfield*

Lewis Research Center

SUMMARY

Three phases of work on a waste-heat ground-test radiator are presented: conceptual design, mechanical design, and fabrication. Based on restrictions of a vacuum-chamber test facility and optimization through the use of a digital computer program, a physical configuration was determined. Construction of the radiator (1000 sq ft outside radiating surface, 40 ft long, 8 ft diam, and 40 finned tubes) was of semimonocoque design for minimum weight and ease of handling. The finned-tube construction consisted of 0.015-inch-wall 316 stainless-steel tubing covered by 0.062-inch-thick 3003 aluminum alloy with diametrically opposite fins of the same aluminum material and thickness. Preformed aluminum panels and tubes were metallurgically joined by more than 1/3 mile of brazed joint. Photographs showing the brazing techniques developed by the fabricator, including the thermal emissivity coating procedure, are included along with the fabrication procedure.

INTRODUCTION

Liquid-metal, Rankine cycle, turbogenerator systems for electric power production in space are inherently complex multiple-loop integrations of many functional components and subsystems, which are usually developed and evaluated in appropriate "workhorse" loop facilities. Although the system performance can be analytically estimated from component characteristics, it is desirable for and expedient to system development to define the performance, control requirements, and operating problems of the

---

*Lockheed Missile and Space Company.

integrated system experimentally over the anticipated spectrum of system and environmental conditions. The flight configuration of the waste-heat radiator, however, is often deferred because its specific design is influenced by either the requirements of a specific mission or the physical constraints of the carrier vehicle or spacecraft or both. Thus, for system development purposes, it is desirable to utilize a radiator that is relatively simple and inexpensive to design and fabricate. In addition, the test radiator must accommodate the limitations imposed by a particular environmental facility. In order to permit an environmental evaluation of a development SNAP-8 power conversion system in an existing facility, the design and fabrication of a flight-weight test radiator for the sodium-potassium heat-rejection loop of the power system was undertaken.

Prior experience in the fabrication of flight-weight, aluminum to stainless-steel, liquid-metal radiators has been associated with systems of much lower power levels (SNAP-2 and SNAP-10A) that required about one-tenth of the necessary radiating surface area for heat rejection of the SNAP-8 system. Fabrication techniques used on the SNAP-10A radiator were not applicable because it had thermoelectric elements between the NaK flow tube and the heat-rejection aluminum fin. The SNAP-2 radiator used a fin-to-tube fabrication procedure whereby a coating of titanium was applied to the L-605 tube in a fused-salt electrolytic bath and then the aluminum fin was brazed to the coated tube in the conventional manner. A casting process (another procedure for bonding aluminum to steel) was being used in making sample armored radiator tubes for the SNAP-8 program. In this process, the steel tube was dipped into a molten bath of aluminum to be cast, in order to tin the surface of the tube. The tinned tube was then placed in a die, and the molten aluminum poured into the die to form the fin. There were two problems associated with this process: (1) a lack of consistency in producing a perfect bond of aluminum to steel and (2) a measurably reduced heat-transfer capability of cast aluminum over that of the brazed joint because the cast aluminum was porous. Both the casting process and the brazing technique were proprietary.

General criteria were established for the design and fabrication of the subject radiator. It was to be an aluminum central fin and aluminum-covered stainless-steel tube configuration that lent itself to a wide variety of fabrication techniques. Also, existing technology and readily available materials were to be used. For economy of weight and size, it is desirable to have the radiator operate at a high radiating efficiency for a given heat-rejection temperature. In order to increase the surface thermal emissivity over that of bare aluminum (0.2 to 0.3, depending on surface condition), an emissivity coating was selected for application on the surface. Much work has been done in developing high-thermal-emittance coatings that have elevated-temperature stability in a vacuum environment. Several inexpensive paint-type coatings that were relatively easy to apply were selected for testing. After extensive testing under conditions that were more

severe than expected, one coating (zinc oxide pigment with a potassium silicate binder) was picked as most acceptable.

Conceptual and mechanical design analysis was performed at the Lewis Research Center. A steady-state analytical design analysis was undertaken by utilizing a digital computer program to define the radiator configuration within the physical limitations imposed by an existing vacuum-chamber test facility and mechanical-design restrictions. Dynamic aspects of test conditions were not considered in the conceptual design. Fabrication and coating techniques used on the radiator by the contractor, Lockheed Missiles and Space Company, that required development are presented in this report.

CONCEPTUAL DESIGN

Physical Limitations

A specific vacuum-chamber test facility dictated the maximum physical dimensions for this ground-test-only waste-heat radiator, even though it was to be flight weight. The chamber (fig. 1) had a 9-foot flanged opening at one end that was to be used for insertion of the radiator. On this basis, a nominal radiator diameter of 8 feet was chosen as a maximum. An investigation of the thermal load capabilities of the 23-foot diameter by 48-foot-long cold wall in the chamber indicated that the heat load could be handled provided it was distributed over the entire cold-wall area. The maximum length of the radiator was restricted to 40 feet as a compromise between the amount of thermal radiation that could bypass the end of the cold wall and the uniform heat distribution over the cold wall.

Mechanical Limitations

An aluminum fin thickness of 0.062 inch was selected because it was a practical minimum which could be extruded by conventional processes and because it was desirable to minimize the distortion of the potentially large fins by giving them some mechanical integrity. The aluminum was to be attached to a 0.015-inch-wall 316 stainless-steel tube selected for its relative strength, minimum weight, compatibility with the liquid-metal eutectic mixture NaK-78 (22 Na - 78 K, percent by weight), and standard wall thickness. Types 3003 and 6061 aluminum alloys were chosen because of their high thermal conductivity. Because the thermal conductivity of aluminum increases with increased temperature, a representative metal temperature was estimated in the following manner: Fin-tip temperature was calculated to be about 0.8 of the fluid temperature. The overall

average metal temperature was then taken as 0.9 of the average fluid temperature. The value of thermal conductivity used was 130 Btu per hour per foot per ^{o}R.

A cylindrical radiator shape was specified for ease of manufacture and to distribute the heat load uniformly over the cold wall, which covered almost 360^{o} of the inside of the vacuum chamber (fig. 1). The finned tubes were manifolded together on both ends so that the NaK would enter the inlet manifold in two places 180^{o} apart, distribute to the tubes in four directions, make a single pass through the tubes, and leave through an identical outlet arrangement on the exit manifold (fig. 2).

Computer Analysis

A number of physical variables were analyzed over a wide range of operating conditions in order to define configuration compromises. To expedite the analysis, a slight modification of an existing FORTRAN digital computer program explained in reference 1 and listed in reference 2 was used. The fin geometry used in references 1 and 2 (a flat-plate central finned tube) is the same basis for radiator design used herein. Meteoroid protection armor on the tube was not taken into consideration, therefore, the aluminum over the stainless-steel tube was specified to be the same thickness as the fin. Although net thermal radiation occurs from the outside of the cylinder to the heat sink, internal radiation and reradiation from one fin to another was accounted for. It was assumed that the test-chamber, cold-wall, heat-sink temperature was 300^{o} R and the temperature of one of the uncooled ends of the vacuum chamber was 500^{o} R, while that of the other end was 700^{o} R.

The design steady-state requirements used in the calculations are listed in table I. An off-design condition of a 19-percent reduction in NaK flow rate with a compensating increase in radiator temperature drop for design heat rejection is also listed in table I. Calculations were performed for both sets of requirements in order to allow the more severe set of conditions to dictate final radiator geometry.

The procedure was to fix the overall geometry of the radiator and to allow the fin thickness be the dependent variable. Results of the calculations shown in figure 3 indicate the effect of tube length and number of tubes on fin thickness, total radiator weight (without the support structure), and outside diameter of the stainless-steel tube (with the maximum pressure drop of 10 psi). For an 8-foot-diameter radiator, ranges of overall length and number of tubes are covered. By using a minimum fin thickness of 0.062 inch, the region of radiator design is markedly reduced. In figure 3(a) and (b) it is seen that, for a constant number of tubes, there is not much to be gained in reducing tube length by using a fin thickness greater than 0.062 inch. The change in fin thickness is much more sensitive than a proportionate change in tube length or number of tubes.

For a constant fin thickness, the required radiator length decreases as the number of tubes is increased.

The off-design condition of the lower flow rate of 34 000 pounds per hour and higher temperature change of 210° R required a larger radiator. Increasing temperature drop across the radiator for a given tube geometry (in order to raise the heat-rejection capacity) increased the fin thickness more than did an increase in NaK flow rate would because of a lower average-radiating temperature. The final radiator configuration selected was based on the off-design condition at increased temperature-drop consideration, since this was the more demanding design. By using the minimum fin thickness of 0.062 inch and a radiator length of 40 feet, a 40-tube configuration was chosen for a heat rejection of 450 kilowatts. This represents about 1000 square feet of outside radiating surface area and results in a total radiator weight (neglecting the support structure) of about 1250 pounds (figs. 3(b) to (d)). The standard tube size (0.375-in. o.d., 0.335-in. i.d.) selected (figs. 3(e) and (f)) was a compromise which gave tube pressure drops of 8 and 12 pounds per square inch at NaK flow rates of 34 000 to 42 000 pounds per hour, respectively.

The effect of the variation of emissitivity on the design point of the selected configuration is shown in figure 4. Reducing the emissivity from 0.9 to 0.5, would reduce the heat-rejection capability from 450 to about 365 kilowatts at the same flow rate and inlet temperature. The design heat rejection capability could be easily and economically be reduced by partially wrapping the radiator with aluminum foil to reduce the effective emissivity of the covered section. Bare, unpolished, oxidized aluminum has an emissivity of 0.2 to 0.3. It is possible to calculate approximately how much length should be covered to attain whatever reduced heat-rejection level is desired.

MECHANICAL DESIGN

Finned-Tube Construction

One of the two problem areas in the mechanical design of the radiator was the construction of the finned-tube, aluminum to stainless-steel joint. A number of different types of joints were fabricated, and a series of environmental tests were conducted to determine the most efficient type of construction for attaching the aluminum fins to the 316 stainless-steel tubes (fig. 5). The bimetal interface between the outside of the stainless-steel tube and the surrounding aluminum sheath is important because the "contact resistance" factor has a strong influence on the efficiency of the heat conduction from the fluid to the fin. The relative thermal-radiating characteristics of various mechanically and metallurgically joined finned-tube samples were evaluated in a vacuum bell

jar. The 4.5-inch-wide samples were fabricated with 1/16-inch aluminum for the 7.5-inch-fin and the conductive material around the 0.375-inch outside diameter by 0.015-inch-wall stainless-steel tube.

A mechanical joint is defined as one in which the aluminum is clamped or shrunk to the stainless-steel tubes, whereas, a metallurgical joint is one in which the aluminum is bonded to the steel tube. The mechanically constructed finned-tube samples evaluated, utilized a shrink fit between the stainless-steel tube and the aluminum fin. This shrink-fit condition was obtained in several ways:

(1) An aluminum fin was machined from a solid bar, and the bore was reamed to a shrink-fit diameter in relation to the outside diameter of the stainless-steel tube, simulating an extruded aluminum fin. After the fin was heated to approximately 1350° R, the stainless-steel tube (at room temperature) was inserted, and the assembly was allowed to cool to room temperature (fig. 5(a)).

(2) A second fabrication method utilized two stamped half-sections that were seam welded to assemble the finned-tube sample. Here, again, the shrink-fit condition was obtained by undersizing the stamped aluminum pieces at the tube section, and by a special clamping arrangement during the seam-welding operation. The shrink-fit condition was obtained after the assembly cooled from the welding operation (fig. 5(b)).

(3) A similar configuration was fabricated by utilizing stampings, but, instead of seam welding, a tungsten - inert gas (TIG) weld seam was made on both sides where the aluminum material surrounds the stainless-steel tube (fig. 5(c)).

(4) Another extruded type fin was machined from a solid block. The tube section of the fin, was split open axially by a thin circular cutter and a V-groove for welding was machined at this open seam. The stainless-steel tube was inserted, and a heliarc weld was made to seal the open junction. The weld pass was made while the fin and tube were assembled in a fixture to produce a "hoop" pressure around the tube. After the weld pass was made, cooling the weld produced the normal material shrinkage in the weld joint, and thus a shrink-fit condition was achieved (see fig 5(d)).

The metallurgical tube-fin joints utilized specialized brazing techniques. For one sample, two stamped half-sections were aluminum brazed to a stainless-steel tube precoated with titanium (fig. 5(e)). Another sample was constructed by a casting process. The aluminum fin was cast around the stainless-steel tube, and then the fins were machined to the proper dimensions (fig. 5(f)). Another braze concept tested was a one-piece fin stamping with the center section formed in a U-shape to accommodate the stainless-steel tube. Braze material was used as a filler around the tube and in the U-section of the fin (fig 5(g)). The open brazed joint was then contour machined to the proper shape.

Evaluation of Fin-Tube Joint

As a standard of comparison, an all-aluminum sample was machined from a solid block with the same inside diameter as the stainless-steel tube (fig. 5(h)). Since no bimetallic interface existed, the conduction of the heat input from the heater rod to the fin was the maximum attainable. The conduction of the bimetallic samples heated to 1160° R by a heater rod in a vacuum bell jar were compared with the all-aluminum standard. All the metallurgical samples compared favorably with the standard, but the mechanically joined samples did not perform as satisfactorily under thermal cycling. Thermal output of most mechanical joint samples decreased after the first thermal cycle. Heating to 1160° R during the first cycle, caused the aluminum surrounding the stainless-steel tube to relax its hoop pressure and allowed the steel and aluminum to accommodate one another. After cooling, only a nonstressed, or slightly stressed, contact remained. When heated to 1160° R in the second thermal cycle, a minute gap existed because the coefficient of thermal expansion of the aluminum material is greater than that of stainless steel. Therefore, the diameter of the aluminum bore section of the fin became larger than the outside diameter of the stainless-steel tube and thus increased the thermal resistance of the bimetal interface.

The finned-tube samples were tested in a bell jar under a vacuum of 10^{-5} torr. A liquid-nitrogen cold baffle absorbed the radiated heat. A sample in the test apparatus is shown in figure 6. Each finned-tube sample was brought to 1160° R (stainless-steel-tube temperature) by a resistance heater inside the stainless-steel tube, and the input power to the sample was measured when the tube reached an equilibrium temperature of 1160° R. Also, the fin surface was instrumented to obtain the radial temperature drop across the fin. All samples had a sandblasted surface finish.

Mechanically joined samples had a power dissipating capacity of 125 to 236 watts per foot, and the metallurgical finned-tube configurations dissipated from 231 to 287 watts per foot, as calculated from the power input.

Coating Tests

The other major design problem was the selection of a coating that would maintain a high thermal emissivity and remain bonded to the substrate material without cracking or spalling at the 1160° R operating temperature and under thermal cycling (25 cycles, estimated startups from room temperature to 1160° R). This phase was accomplished by conducting tests on seven different coatings that appeared to meet the coating requirements. Aluminum squares, 1-inch by 1-inch by 60 mils thick were machined to ensure flatness, and the underside edges were beveled on a 45° angle. Several aluminum

squares were sprayed with the same test paint. Each square was coated to approximately 5±1 mil. A copper platen was machined with provision for tubular heating elements to be embedded in this hot plate for heating the samples to 1160° R. A 1/2-inch-outside-diameter copper tube was brazed onto the bottom of the copper platen in an S-shaped configuration. The purpose of the tube was to air cool the platen and paint samples conductively to room temperature quickly. This cooling would produce a mild thermal shock to the coating.

Several paint samples were individually temperature instrumented, bolted onto the instrumented platen, and placed in a bell jar. The samples were heated to 1160° R in about a 1/2 hour and then returned to 530° R in about 5 minutes. Twenty-five cycles of this nature were conducted. The various paint samples, after the first and twenty-fifth heating-cooling cycles, respectively, in a vacuum between 10^{-5} to 10^{-6} torr, are shown in figures 7(a) and (b). After the second and third cycles, most of the coating started to crack and blister, and the original white color took on a gray or beige cast. The coating that best survived this thermal cycling (ref. 3) was a zinc oxide coating, Z-93, a zinc oxide pigment with a potassium silicate binder (developed at Illinois Institute of Technology Research Institute). This material remained bonded to the aluminum and underwent a slight color change from the original snow white to an eggshell shade. In addition to the thermal cycling, an endurance test was conducted at 1160° R for 16 hours (two 8-hr periods). Here again the Z-93 coating remained stable, only undergoing a slight color change.

Since the radiator was intended for use in an environmental facility and, hence, would not be subjected to a solar ultraviolet-radiation environment, which would tend to degrade the coating, slight changes in color were not critical. The coating was, therefore, selected solely on the basis of high thermal emissivity and adherence to the metal.

Samples of the Z-93 coating were prepared by Lockheed with their production techniques. Thermal-emissivity values of some of the test specimens were checked prior to preheating, for others, after they had been cycled 25 times, and for several of the specimens, subsequent to endurance tests for 16 hours in two 8-hour cycles. The apparatus and the method used for checking the thermal emissivity of the test specimens are described in reference 4. Repeatability of emissivity measurement in these tests was within ±1 percent. Table II shows the effect of temperature and thermal cycling on thermal emissivity of seven Z-93 coating samples. These values have been rounded off to the nearest 1 percent. Only sample 1 had a high value of emissivity at room temperature before it was cycled, but it is included because it was the only sample tested to 1075° R. Sample 2 was checked for the first three cycles and the values were repeated. Samples 3 to 7, which had either been cycled 25 times or heated at 1160° R for 16 hours, indicated that the thermal emissivity had increased slightly.

Because the Z-93 zinc oxide coating performed best and because the application of the coating to the aluminum fin appeared to present no insurmountable problems, it was selected for the radiator fin coating.

Radiator Support Structure

Type 304 stainless steel was selected for the support structure because it has a minimum outgassing characteristic in a vacuum environment, a high working stress at elevated temperatures, and is readily available in pipe, tube, and plate forms.

The detailed configuration of the support structure was dictated by the working stress of the 0.375-inch-diameter, type 316 stainless-steel NaK conveying tubes. The aluminum fin section surrounding the tube was not considered as adding to the section modulus of the finned-tube configuration, since it would be operating near the annealing range of aluminum. The flexural stress of the stainless-steel tube, was limited to about 13 000 pounds per square inch (below the ASME Boiler Code maximum working stress of 17 000 psi), necessitating a support spacing of 4 feet. This dimension was also a convenient spacing for the overall 40-foot-assembly length. Since circular supports were required every 4 feet and a method of fastening the finned-tube sections to the supports was required, a Z-shaped cross section was selected for the circular frames to facilitate the required bolting, which is shown in detail in figure 8.

Because of the difference in heating and cooling rates and the differing coefficients of thermal expansion for the finned tubes and the support structure, it was necessary to provide unrestrained relative motion in the longitudinal direction for these components. This motion was achieved by providing slots in the fins and by fastening the fins with shoulder bolts through these slots. The 11 Z-shaped circular frames were supported by two 8-inch-diameter, schedule 10, 40-foot-long stainless-steel pipes on both sides (fig. 9).

The two main 8-inch-diameter pipe supports of the structure were joined together with five $3\frac{1}{2}$-inch diameter, schedule 10, stainless-steel pipe sections spaced approximately 10 feet apart. The 11 Z-shaped circular frames, 8 feet in diameter, were supported by the two main 8-inch-diameter supports. The circular frames were welded to the pipe sections in conjunction with special shaped gussets. The Z-shaped circular frames were tied together with six hat-shaped sections, spaced 45° apart, running longitudinally, similar to stringers in an airframe.

The 40-foot-long finned tube assemblies were fastened to the Z-shaped formers by special shoulder bolts through the insulating blocks of an asbestos fibre, diatomatious silica composition to eliminate conductive heat transfer from the finned-tube assemblies to the structure. Because differential expansion would be involved, the midpoint of each

finned-tube assembly was fixed and each end was allowed to float in relation to the structure.

In the design of the required fastening slots in the finned-tube assemblies, consideration was given to the possibility that the power system would be cold soaked before a startup would occur. Under this condition, the radiation temperature would approach the liquid-nitrogen cold-baffle temperature in the environmental test chamber and, hence, the assemblies would contract. Because the aluminum-fin steel-tube assemblies would contract a greater amount than the stainless-steel structure, a slot allowance (fig. 9) had to be made in the fin surface at each bolting point to allow for the 140° R condition. Upon startup of the system and initial flow of the NaK fluid, the finned-tube assemblies would expand a greater amount than the structure thus requiring the slots in the fin surfaces to accommodate the change from the 140° to the 1110° R operational condition.

Three support legs on each side provided a center-to-center support span distance of 20 feet for the 8-inch pipe section, as shown in figure 9. The structure was designed to be lifted by two support points on half the radiator, allowing the other half to cantilever and enter the environmental chamber through the 9-foot-diameter door. With half the radiator inside the chamber, the supporting legs with rollers would be installed, thus allowing movement on the interior tracks in the chamber and insertion of the other half of the radiator.

The weight of the radiator assembly (without the support legs) was approximately 3600 pounds; the structure accounted for 2350 pounds; and the finned tubes with associated plumbing 1250 pounds.

FABRICATION

The general plan for manufacture of the radiator by Lockheed Missiles and Space Company called for separate fabrication of support structure, finned-tube assemblies and inlet and outlet headers. These components were then brought together for a final assembly operation in which headers and feed lines were positioned on the support structure and welded to the radiator tubes and headers. The complete assembly was then packaged for transportation by truck.

Radiator Assembly

The headers presented no unusual fabrication problems; however, special procedures for brazing, tube joining, and surface coating had to be developed into controlled shop processes before the manufacture of the finned-tube assemblies could be accom-

plished. The following discussion describes the essential details of the fabrication-procedure development.

Selection of Tube-to-Fin Joining

Primary fabrication requirements for the tube-to-fin joint were (1) that it permit adequate heat transfer and (2) that economy in fabrication time and facilities be attained without a special process development phase. These requirements were set in order to keep the cost to a practical minimum, which implied that a mechanical joint could be used in the event that a metallurgical joining process was not readily attainable. The casting process and the brazing techniques explained in the INTRODUCTION were not used because these methods were of proprietary nature.

Three mechanical and two metallurgical (brazed) segments of tube-to-fin assembly were fabricated and tested for heat-transfer characteristics (fig. 10). Any segment was considered to be satisfactory from the standpoint of manufacturing economy. Specimen fin length was 12 inches, and the tubing was allowed to project 2 inches from either end. Results of heat-transfer tests on the five joints are shown in figure 10, where heat-rejection rates in watts per foot are plotted against tube wall temperatures. Comparisons shown here indicated that a mechanical joint would not be satisfactory for the radiator. Although the spring joint showed potential heat-transfer capability equivalent to that of the type B brazed joint (fig. 10), its thermal resistance was evidently sensitive to spring pressure, thus, precision fitting was required for predictable results.

Of the two brazed joints, the one designated type B (fig. 10) was selected for production of the radiator. This configuration showed adequate capacity for heat transfer and was more economical to fabricate. Qualification of this joint was further verified by thermal cycling 25 times from 560° to 1210° R, which indicated no loss in heat-transfer characteristics.

Development of Tube-to-Header Joint

The most critical operation in fabrication of the radiator was joining the thin-walled tubes to the end headers. Details of the joints that were developed are revealed in figure 11. The primary operation was to flare the ends of the radiator tubes to a diameter approximately 30 percent greater than that of the basic tube. The flared ends accommodated a special fitting machined for a light press fit into the flare. In this manner, joint welding, which involved the tubing, was performed automatically in a precision jig without fear of burnthrough due to the relative massiveness of the fitting.

Three test specimens were used in tube-to-header joint development. Two of these ruptured by the application of internal pressure, while the other ruptured by longitudinal tension loading. Rupture stresses were as predicted for the 316 stainless steel. To achieve a high quality of joint, it was necessary that a great deal of attention be paid to design of the flaring tool and to preparation of the tube ends prior to flaring. Precision-ground die and mandrels, chromium plating of sliding components, positive stops on the mandrels, and trial-and-error design of the proper forming radii were all necessary steps in achieving the results shown in figure 11(a). The cross section in figure 11(b) shows the final assembly weld made between the tube end fitting and the header manifold fitting. The design was such that only a fillet weld in heavy walled sections was required, thus, practically eliminating a chance for burnthrough at final assembly.

Production of Brazed Assemblies

The production line for manufacture of the brazed finned-tube assemblies is shown in figure 12. Forty 40-foot units were produced for the radiator, requiring 1600 feet of brazing. Figures 13 to 15 show successive key steps.

The first operation was to prepare the tube. Fifty-foot pieces were cut to the proper length, the ends flared and fittings were welded on by an automatic process. The outside tube surface was then pretinned (fig. 13) with a no. 718 aluminum brazing alloy, which has a melting point of 1530° to 1540° R. The composition is as follows: silicon, 11.0 to 13.0; copper, 0.30; iron, 0.80; zinc, 0.20; magnesium, 0.10; and manganese, 0.15 percent; with aluminum constituting the remainder. This alloy was also used to make the tube-to-fin joint. The welding station and the series of tube supports used during welding and precoating are shown in figure 12. The special tooling devised for pretinning is shown in figure 13. A motor-driven carriage, which traveled along special tracks paralleling the tube, supported an air-motor-driven (600 rpm) stainless-steel wire brush to roughen the surface of the tube, an acetylene torch, and a rod of brazing alloy. The carriage traveled at 12 inches per minute. At the same time, the tube was rotated at 200 rpm by a motor drive at the end of the production line. The tube was heated to approximately 1650° R by the torch so that a molten zone of coating material 5 mils thick was created in the vicinity of the wire brush. By scarifying the stainless-steel-tube surface in the presence of molten aluminum brazing alloy, a metallurgical bond was created with the stainless steel. The texture of the brazed coating and its thickness were controlled through adjustment of tube rotation, carriage speed, and flame temperature.

After a tube was prepared in this manner, the fins could be joined. For this operation, the special brazing fixture shown in figure 14 was made. Preformed fin segments

approximately 4 feet long were positioned on the bed of the tool and brought within 100° R of the brazing temperature by heat applied with electrical resistance heaters on the underside of the fin. The bed temperature was 1450° R. A tube that had been prepared, as described previously, was then placed in the preformed groove and held in position by spring-loaded plungers. Pellets of the 718 alloy brazing were then deposited on the tube joint to be melted and to form an aluminum cap over the tube and fin. As shown in figure 14, this phase of the operation was performed manually. The necessary brazing heat above that available from the tool was supplied by hand acetylene torches. This operation took 25 minutes. An enlarged section through a typical production joint for the radiator is shown in figure 15. This sample of work was taken from one of several process control panels that were made during the course of manufacturing the finned-tube assemblies.

After brazing was complete for a 40-foot unit, the fin edges were trimmed straight and parallel to avoid interference at final assembly. At the same time, the attachment slots were routed by using a special template to ensure proper matching with the mounting blocks on the support structure rings.

As a final operation in producing the brazed assemblies, the excess deposit of filler metal was removed by milling (fig. 16). The surface emissivity coating applied in a subsequent step was inorganic, and, to prevent surface contamination, no organic coolants were permissible for the milling cutters. All organic coolants contaminated the surface of the finned tube and were difficult to clean satisfactorily prior to the coating operation. Water was used as the coolant for all milling work. The braze-fill contour shown in figure 8 was produced in a single pass.

Coating and Protecting Finned-Tube Assemblies

After brazing and trimming, application of the emissivity coating and installation of the protective and stiffening covers on each 40-foot unit remained to be done. The sequence of operations involved are shown in figures 17 to 19.

Preparation of fin surfaces for coating began with methyl ethyl ketone washing to remove finger prints and other contaminants. This step was followed by successive treatments involving scrubbing with an abrasive cleanser, steam cleaning, and sandblasting with fine aluminum oxide grit. A water-break free-surface condition with a lightly abraded texture was produced. The coating was applied within 8 hours after surface preparation was completed.

The emissivity coating Z-93 was applied in a special air-conditioned room to prevent contamination with organic particles. The surface material being applied to a 40-foot unit is shown in figure 18. A standard spray gun with a 1-liter reservoir was

used. The zinc oxide pigment tended to settle rapidly. Shaking the pigment by hand was the most satisfactory means of maintaining a proper mixture. The coating was applied in four light passes with brief drying between each pass. Final drying required 48 hours in room-temperature air.

After the emissivity coating was dry, each fin segment was individually wrapped with polyethylene sheeting and sealed on all edges. This covering, which provided protection for the radiating surfaces, remained in place as part of the final packaging of the radiator assembly.

A final step in manufacture of the 40-foot units was the attachment of the continuous, full-length, plastic hat section to provide stiffness for subsequent handling. This cover was also part of the final packaging that provided stiffness against vibratory motion, which could be introduced during transport. Figure 19 shows the packaging operation in detail.

Production Inspection For Quality Control

The four inspection steps in the manufacture of the 40-foot finned-tube assemblies to assure satisfactory quality for the radiator are as follows: (1) tube-end flaring, (2) automatic welding of tube-end fittings, (3) brazing of fins to tube, and (4) application of the emissivity coating. The most critical fabrication detail in the radiator was the tube-to-header joint. Inspection of this joint began with the flaring operation. Each flared end was studied under magnification to detect any splitting of the tube wall that could occur if the tube ends were not sufficiently smooth prior to expansion. Also, random defects in the form of longitudinal die marks or voids originating in a starting ingot could appear in the tube wall which, if present in a zone of flaring deformation, could lead to cracking. After end fittings were welded in place, each tube end was X-rayed. Less than 2 percent of the welded joints were returned for rewelding.

Final proof of joint quality came after the brazing was completed but prior to spray coating when a helium leak check of the entire length of each 40-foot unit was performed. The tube was pressurized with helium at 15 pounds per square inch gage, and the sensing device, set for a sensitivity of less than 1 part per million of helium, was used for inspection. No leaks were delected in these separate subassemblies. The absence of leaks was later verified by a final leak test of the complete radiator.

Control of the quality of fin-to-tube brazing was accomplished by a sampling procedure. A 4-foot assembly for every four production units was produced for destructive inspection in a process control laboratory. These specimens were prepared in the production brazing tool under conditions identical to those experienced in manufacture. The 4-foot-long sample was cut into 1-inch segments and microscopically inspected.

Inspection of the Z-93 emissivity coating procedure was performed by spraying samples during the production spraying. Test panels were prepared with each pair of 40-foot units and subjected to a thermal-cycling treatment. After 25 cycles in air from room temperature to 1160° R, there was no cracking, blistering, or delamination of the surface.

SUPPORT STRUCTURE

Fabrication of the support structure was straightforward, and no unusual problems were encountered in its manufacture. The completed structure is shown in figure 20 preassembled for a fit-up of the three pairs of legs. After this operation, the legs were removed and the cylindrical portion of the structure was mounted on special support cradles, which served during all subsequent manufacturing and transportation phases. AISI 304 stainless steel was used throughout.

FINAL ASSEMBLY, PROOF TESTING, AND SHIPPING

Figure 20 shows how the radiator components were assembled around the support structure. Header manifolds were first clamped into temporary position at both ends and main flow piping was welded in place. All the 40-foot finned-tube units were then bolted loosely into position on the support rings. Asbestos-type insulating blocks, which formed mounting points for the fins on the support structure shown in detail in figure 9, are shown in figure 20. After the 40 finned-tube assemblies were in place, their end fittings were mated with corresponding fittings on the header manifolds and a joint was formed by manual welding. This weld was described previously and shown in figure 14(b). The assembly operation was then completed by tightening all supporting fasteners. Proof tests by hydrostatic pressure and helium leak check were conducted on the completed radiator. A radiographic inspection of the final assembly weld was also performed by using the radioactive isotope iridium 192 as a source. The radiator, as it was rigged for loading, is shown in figure 21.

Protective coverings consisting of two end bulkheads and a canvas shroud were supported from full-length side rails (fig. 21). The radiator and support structure were isolated dynamically from the truck bed by rubber shear mounts inserted between the support cradle and side rails. Vibrations of the load were picked up by special instrumentation mounted on each end bulkhead and continuously monitored in the truck cab. Final leak test at the delivery point showed that no damage had occurred during shipping.

CONCLUDING REMARKS

A ground-test waste-heat radiator with 1000 square feet of outside surface for test of a mercury Rankine cycle power system was conceptually designed by use of a digital computer program. Even though a type of aluminum to stainless-steel finned-tube configuration was specified that lent itself to a wide variety of fabrication techniques, some development of an aluminum to stainless-steel joining procedure was necessary.

Lewis Research Center,
National Aeronautics and Space Administration,
Cleveland, Ohio, November 28, 1966,
701-04-00-02-22.

REFERENCES

1. Saule, Arthur V.; Krebs, Richard P.; and Auer, Bruce M.: Design Analysis and General Characteristics of Flat-Plate Central-Fin-Tube Sensible-Heat Space Radiators. NASA TN D-2839, 1965.

2. Auer, Bruce M.; and Saule, Arthur V.: Computer Program Details for Design of Sensible-Heat Space Radiators. NASA TN D-2840, 1965.

3. Zerlaut, Gene A.; and Harada Y.: Stable White Coatings. Rep. No. IITRI-C207-25 (NASA CR-52134), IIT Research Institute, Aug. 27, 1963.

4. Curtis, Henry B.; and Nyland, Ted W.: Apparatus for Measuring Emittance and Absorptance and Results for Selected Materials. NASA TN D-2583, 1965.

TABLE I. - RADIATOR CONDITIONS USED

IN COMPUTER ANALYSIS

Condition	Design	Off-design
Heat load rejected, kW	450	450
NaK flow rate, lb/hr	42 000	34 000
Inlet temperature, ^{o}R	1125	1125
Outlet temperature, ^{o}R	955	915
Pressure drop, psi	10	10

TABLE II. - EFFECT OF TEMPERATURE AND THERMAL CYCLING ON

THERMAL EMISSIVITY OF Z-93 COATING SAMPLES

Sample	Previous heating	Cycles	Temperature, ^{o}R						
			540	705	860	930	1010	1075	540
			Emissivity						
1	None	1	0.95	----	----	0.92	0.89	0.87	----
2	None	1	0.92	0.95	0.93	0.91	0.90	----	0.91
		2	.91	----	----	----	.91	----	.91
		3	.91	.93	.93	----	.91	----	.91
3	25 Cycles	26	0.95	0.98	0.98	----	0.95	----	0.94
		27	.94	----	----	0.96	----	----	.94
4	25 Cycles	26	0.94	0.97	----	----	----	----	0.94
		27	.94	.97	0.96	----	0.95	----	.94
5	25 Cycles	26	0.95	0.98	0.97	0.96	0.96	----	0.95
		27	.95	.97	.96	.96	----	----	.95
6	16-hr endurance	3	0.95	0.98	0.97	0.96	0.96	----	0.95
7	16-hr endurance	3	0.94	0.97	0.96	0.95	0.95	----	0.94

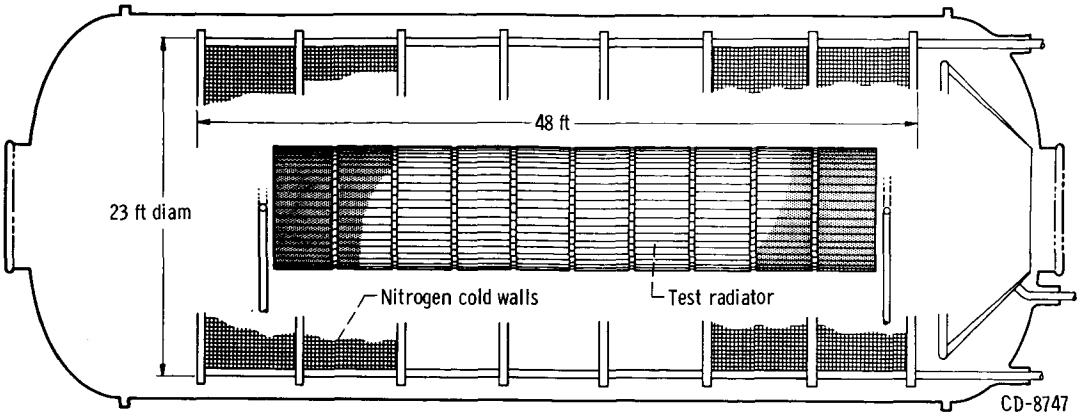

Figure 1. - Installation plan for SNAP 8 ground test radiator in environmental test chamber.

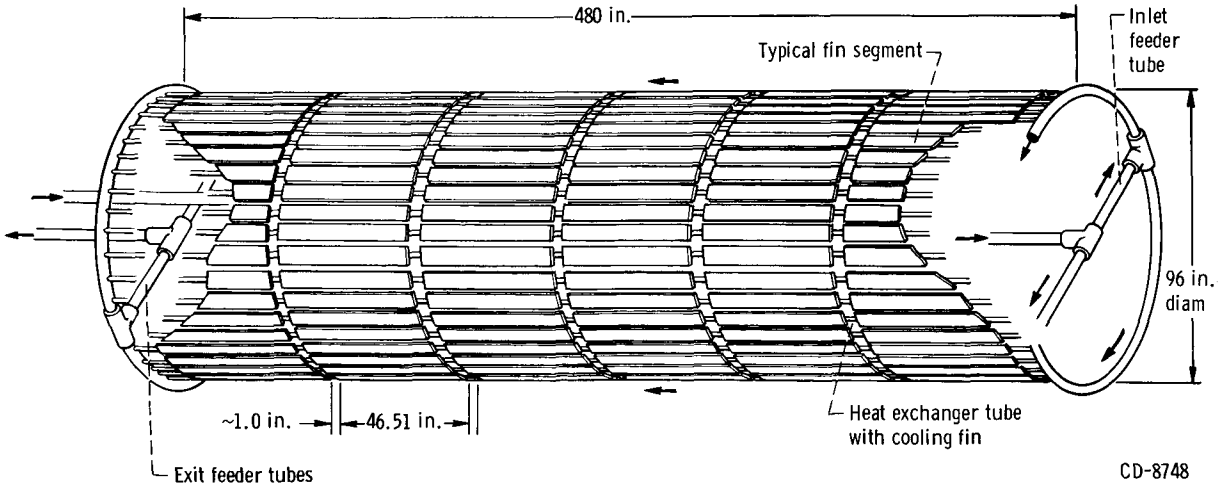

Figure 2. - Radiator-finned-tube header arrangement without support structure. (Arrows denote NaK flow direction.)

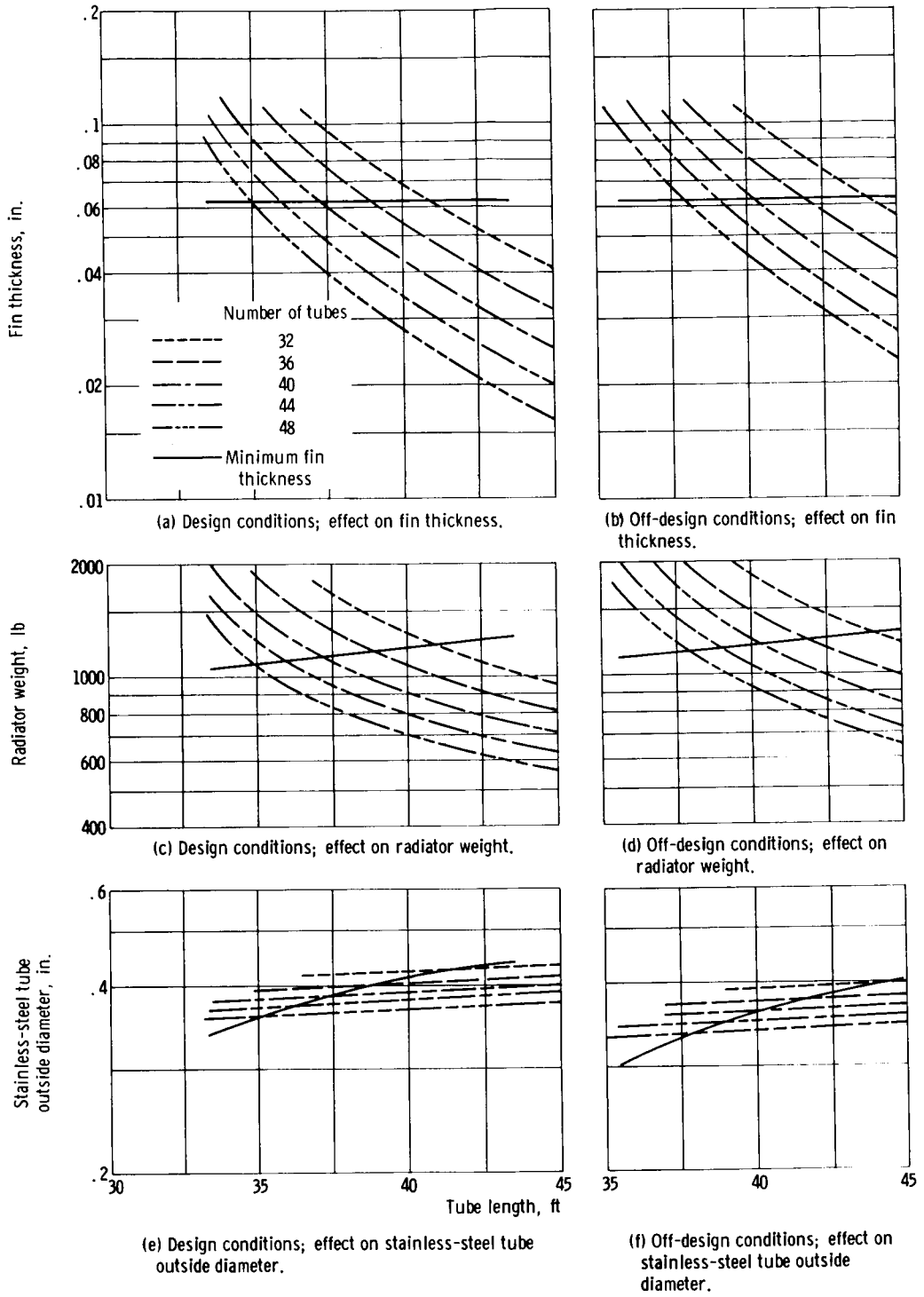

(a) Design conditions; effect on fin thickness.

(b) Off-design conditions; effect on fin thickness.

(c) Design conditions; effect on radiator weight.

(d) Off-design conditions; effect on radiator weight.

(e) Design conditions; effect on stainless-steel tube outside diameter.

(f) Off-design conditions; effect on stainless-steel tube outside diameter.

Figure 3. - Effect of variations in number of tubes and tube length (see table I).

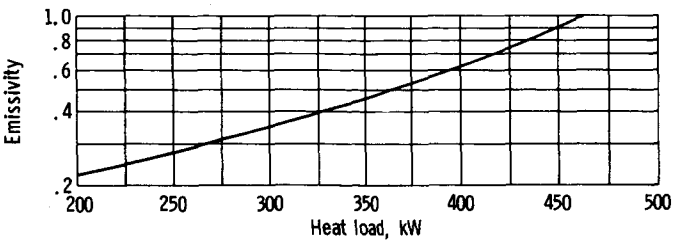

Figure 4. - Effect of changing emissivity on heat-rejection capability of final-design radiator.

(a) Simulated extruded fin and sheath shrunk on stainless-steel tube.

(b) Stamped overlaping half-sections seam welded over stainless-steel tube.

(c) Stamped half-sections tungsten-inert-gas welded over stainless-steel tube.

(d) Simulated extruded fin split and then tungsten-inert-gas welded after stainless-steel tube insertion.

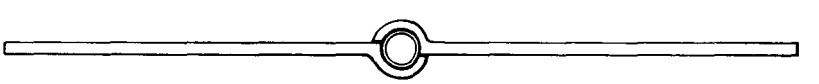

(e) Stamped half sections aluminum brazed to stainless-steel tube, precoated with titanium.

(f) Aluminum material cast around stainless-steel tube with fin welded to aluminum casting.

(g) Stamped full fin brazed to coated stainless-steel tube with part of tube covered with braze material.

CD-8749

(h) All-aluminum finned-tube size machined from solid block used as reference for heat-rejection tests.

Figure 5. - Schematic drawings of sample finned-tube joints for testing.

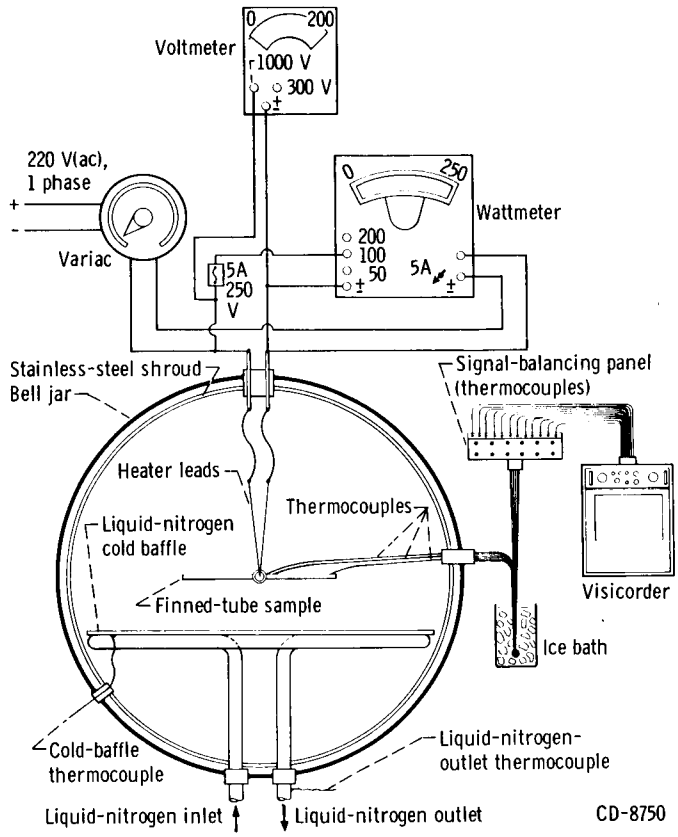

Figure 6. - Schematic drawing of finned-tube sample in heat-rejection test apparatus.

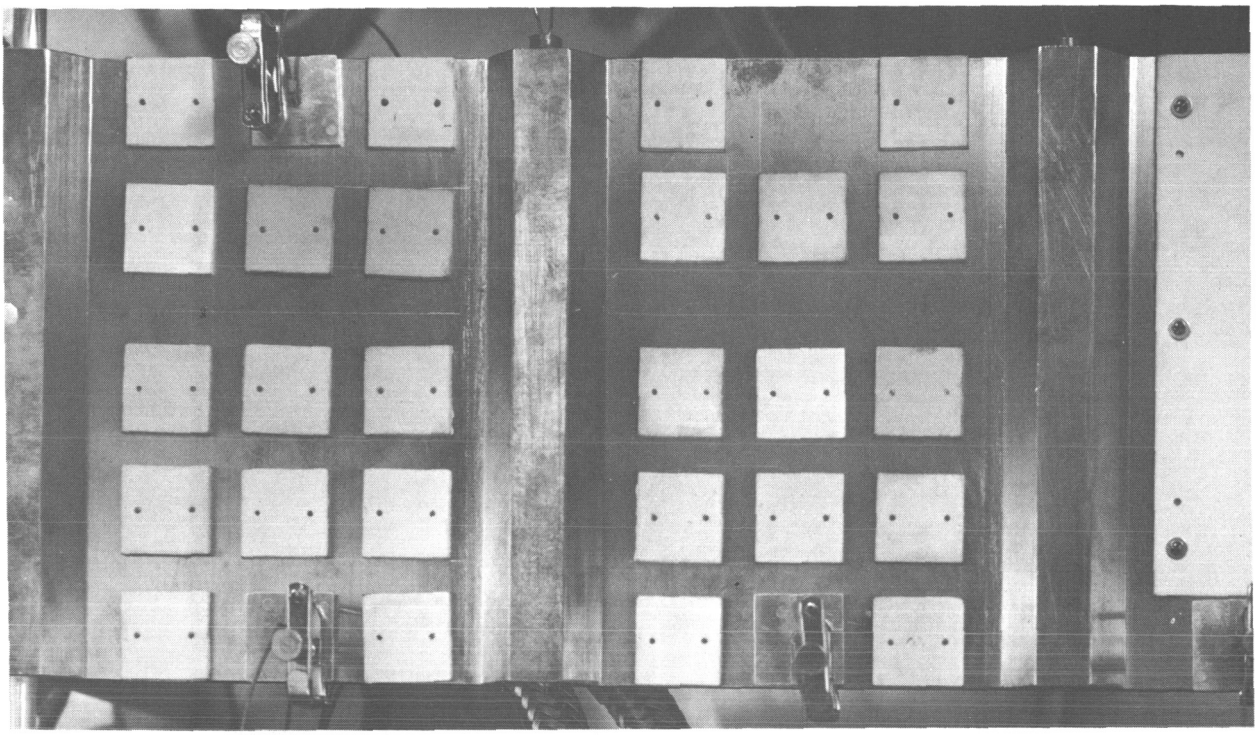

(a) After first cycle.

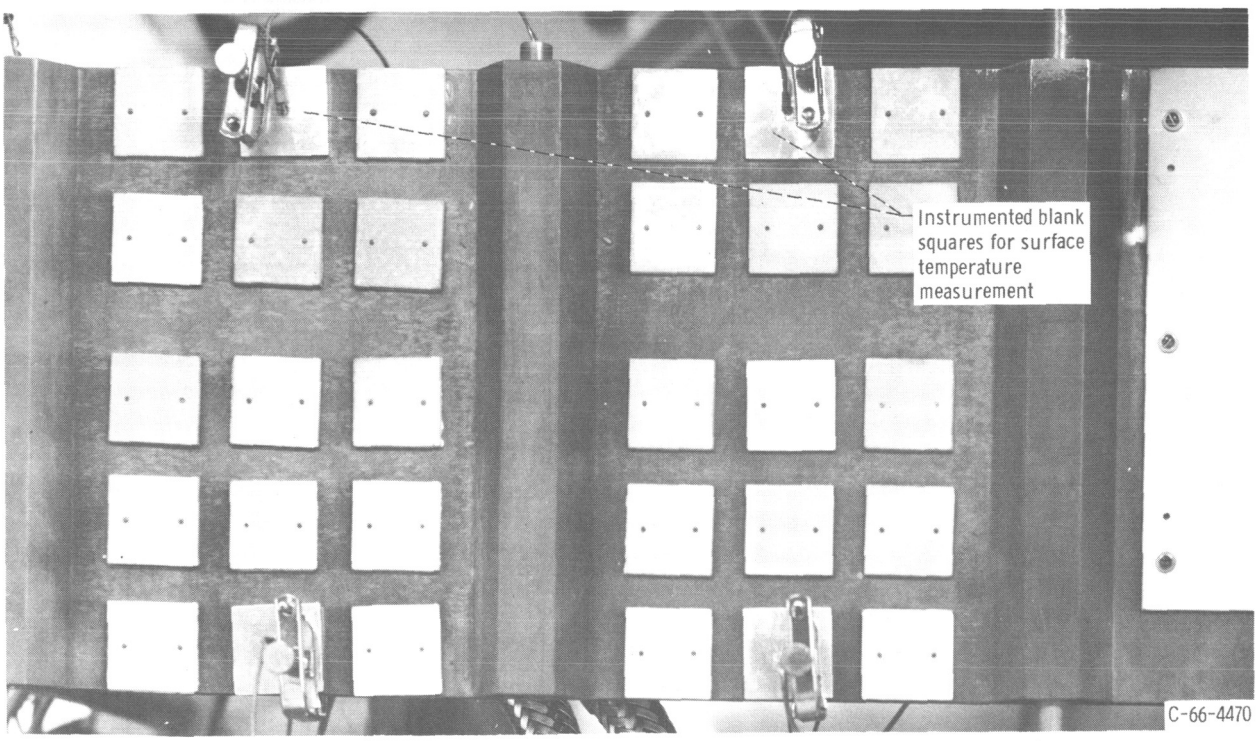

(b) After twenty-fifth cycle.

Figure 7. - Paint samples after thermal cycling.

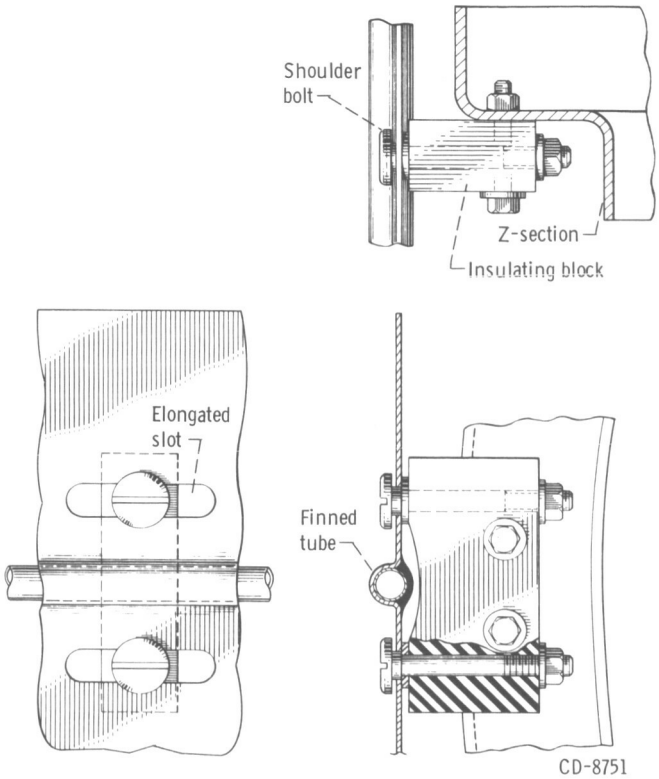

Figure 8. - Detail of finned-tube attachment to Z-shield circular frame.

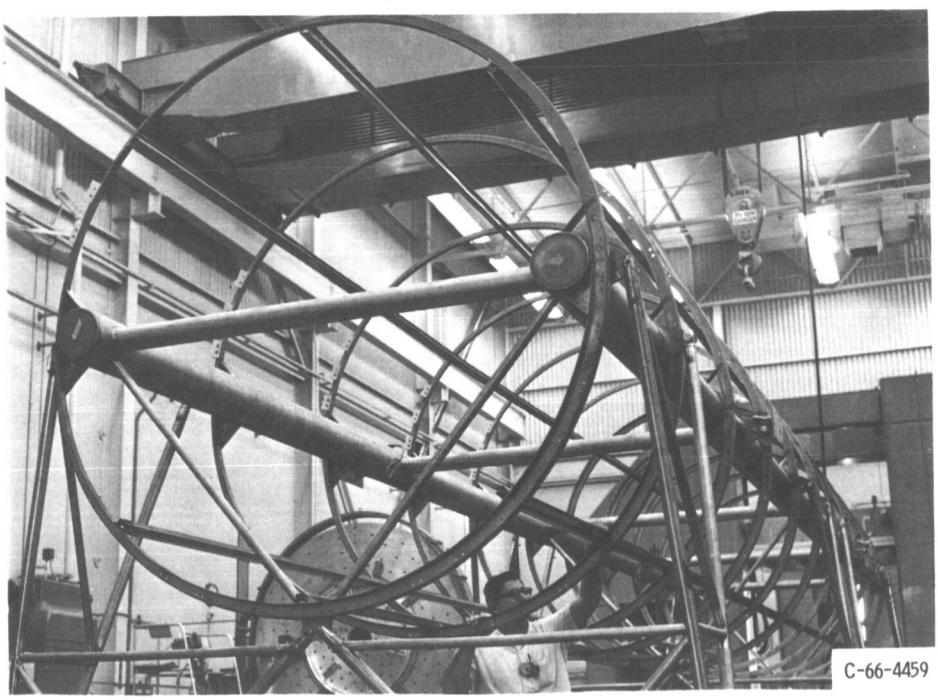

Figure 9. - Preliminary assembly of support structure showing 11 Z-shaped circular frames.

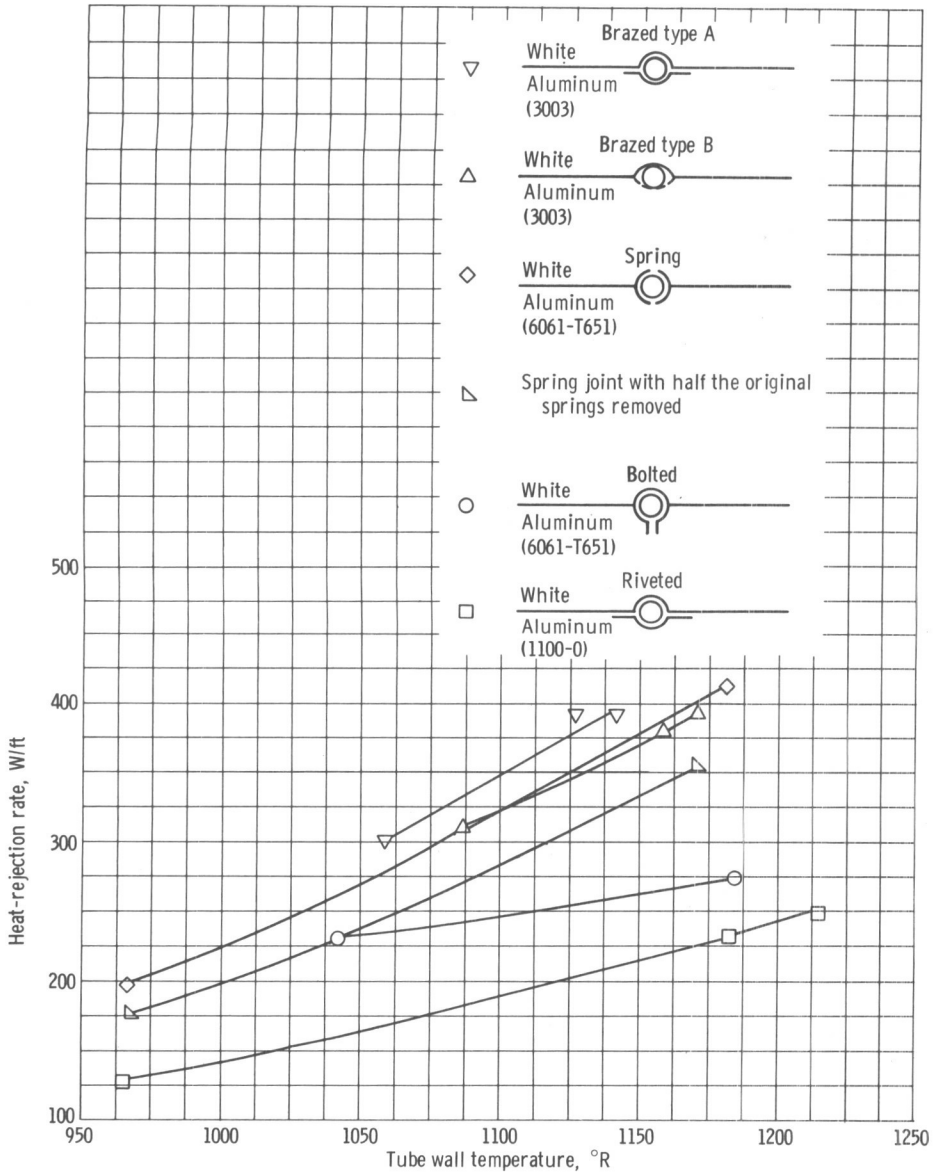

Figure 10. - Experimental heat-transfer rates as function of temperature of tested finned-tube samples.

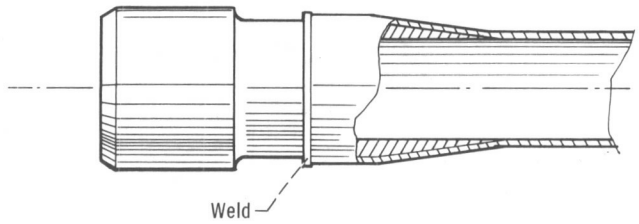

(a) Flared tube on special machined tube fitting.

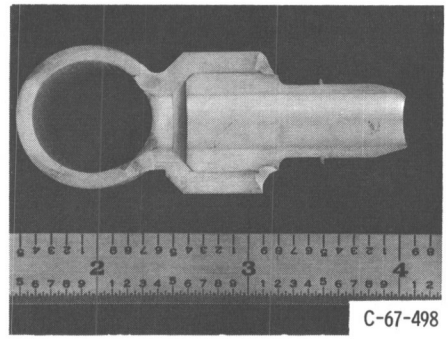

(b) Final hand-welded joint between header manifold and tube end fitting.

Figure 11. - Details of tube-to-header joints.

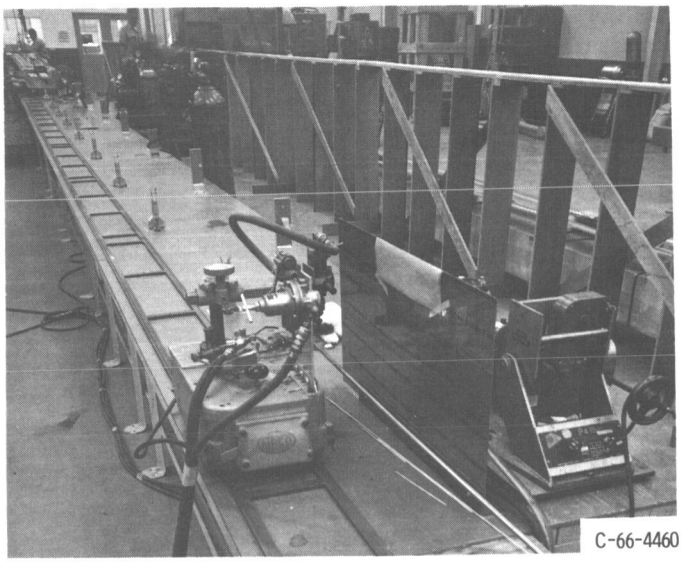

Figure 12. - Production line for manufacture of 40-foot finned-tube assemblies.

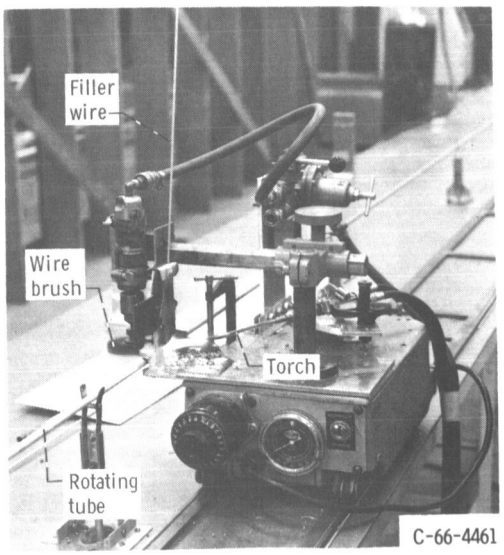

Figure 13. - Detailed view of pretinning operation for finned-tube assembly.

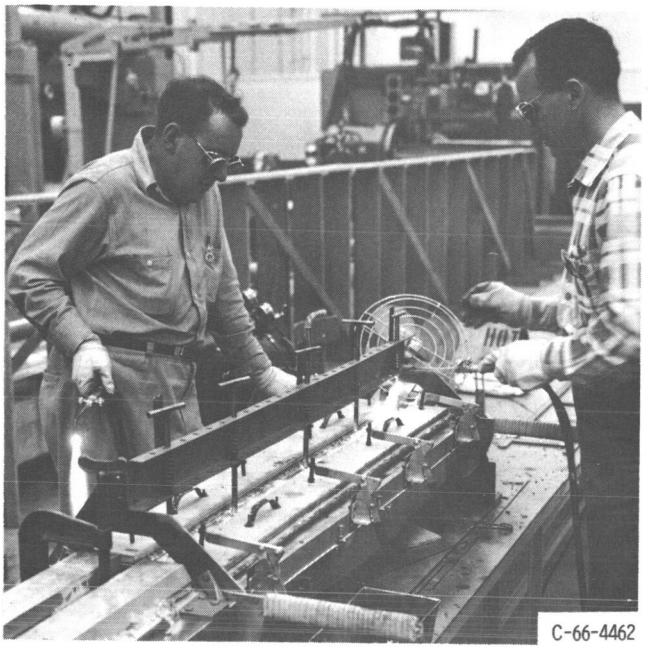

Figure 14. - Brazing fixture for manufacture of finned-tube assemblies.

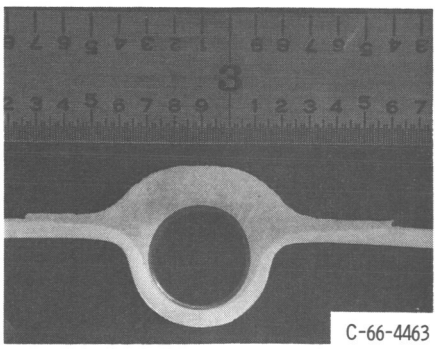

Figure 15. - Brazed fin and tube.

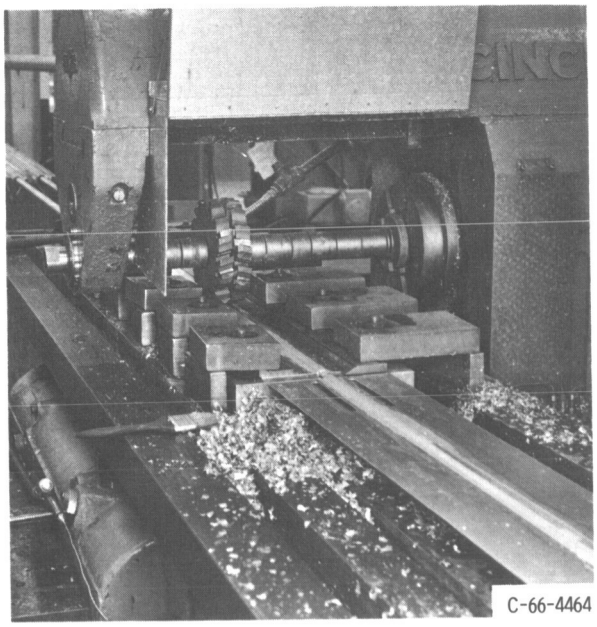

Figure 16. - Removal of excess braze filler by milling.

Figure 17. - Sandblasting a 40-foot finned-tube assembly prior to spray coating.

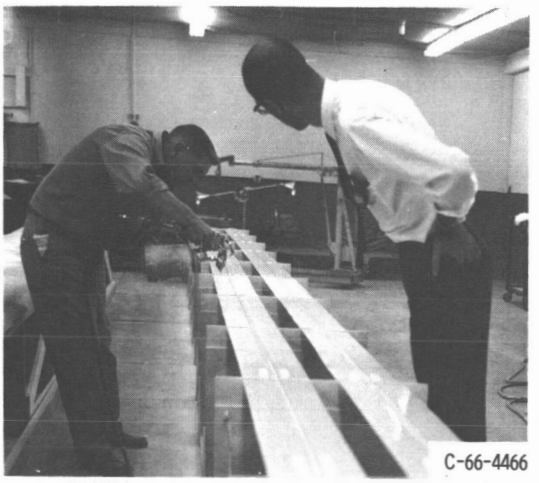

Figure 18. - Application of Z-93 coating to two 40-foot finned-tube assemblies.

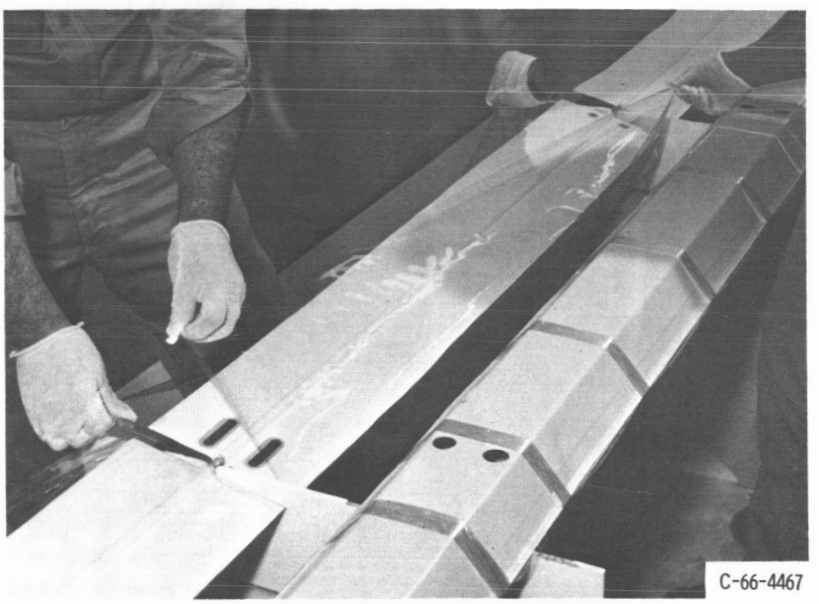

Figure 19. - Packaging operation showing protective plastic sheeting and stiffening members being placed on fins after spray coating.

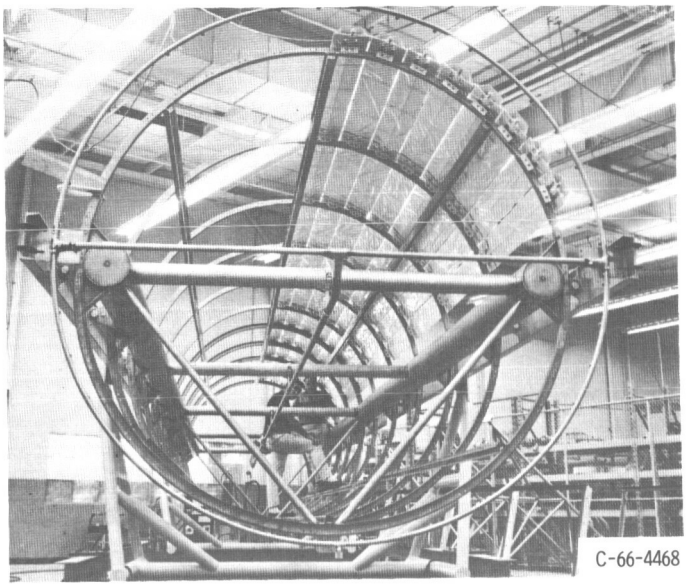

Figure 20. - Assembly of finned tubes on support frame.

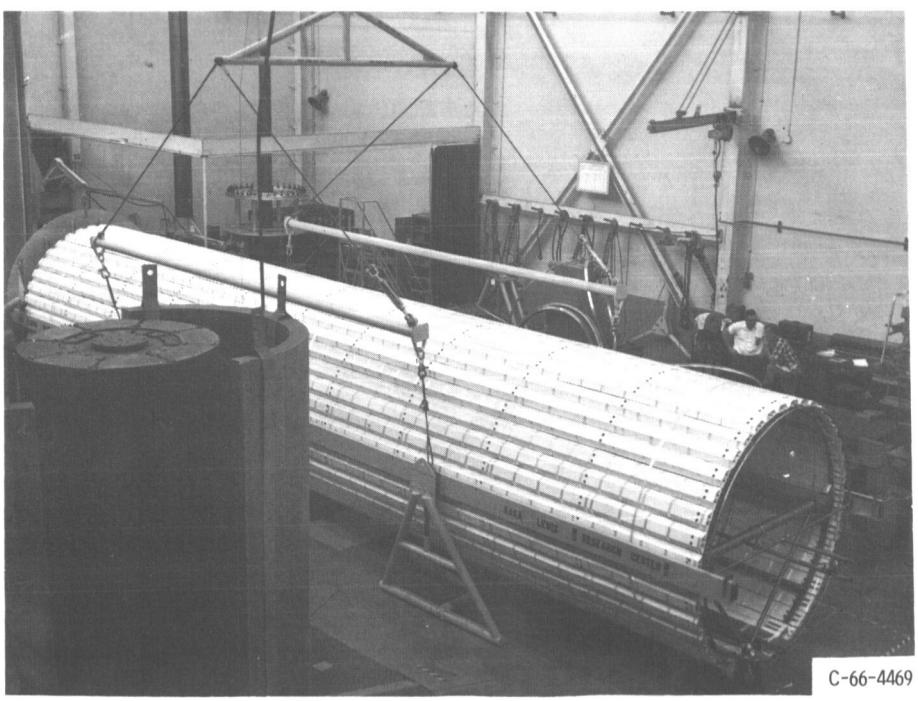

Figure 21. - Final radiator assembly on support cradles rigged for lifting.

NASA-Langley, 1967 —— 11 E-3587